Velocity Potential As a Tool To Diagnose ENSO-Related Circulations

Introduction

According to Gill et al. (2015), velocity potential anomalies are used as a surrogate for regional divergence or convergence aloft during El Niño seasons. Because ageostrophic winds vary with the horizontal gradient of velocity potential, the velocity potential is a deconstruction of the irrotational winds, representing divergence aloft and ascent throughout the column. At 200 mb, warm SSTs in the central and eastern Pacific during El Niño are accompanied by positive velocity potential anomalies aloft over the Indian Ocean region and negative anomalies over the eastern equatorial Pacific.

Relevance to Nuclear Niño

In the aftermath of the 150 Tg black carbon injection there is a rapid descent into an El Niño state in simulations with the earth system model CESM1(WACCM4), as seen in the change in the Southern Oscillation Index (SOI) in Figure 1. Velocity Potential (VP) at 200 hPa (VP200) can be used as a diagnostic tool for the upper level divergence through computation of the irrotational winds.

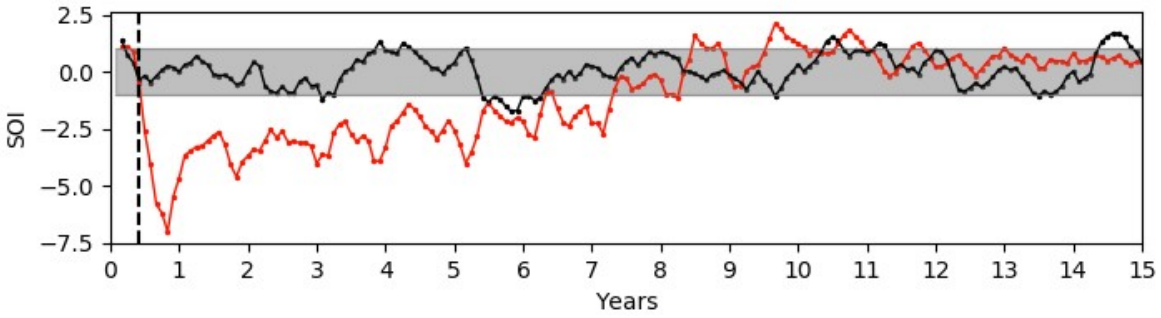

Figure 1. Southern Oscillation Index following the injection of 150 Tg of black carbon over the US and Russia (red) compared to the control run (black) during the same time of year.

The injection takes place on 0005-05-15. The VP200 anomalies in the 3 months prior to the nuclear war indicate La Niña-like conditions with upper level convergence over the Maritime Continent and Australia (see Figure 2a). The 3-month averaged VP200 anomalies centered on 0005-05 through 0005-09 are shown in Figure 2b-f. Figure 2 shows that the signal of positive VP200 anomalies (enhanced upper level convergence or sinking air) originates near Africa and moves eastward towards the Maritime Continent and Western Pacific Ocean. Positive VP200 anomalies in the vicinity of the Maritime continent are indicative of an El Niño-like state in the atmosphere. This provides support for the hypothesis of Khodri et al. (2017) which suggests that eastward propagating Kelvin waves originating from equatorial Africa are suppressing convection in their wake, contributing to westerly wind anomalies as they approach the Maritime Continent.

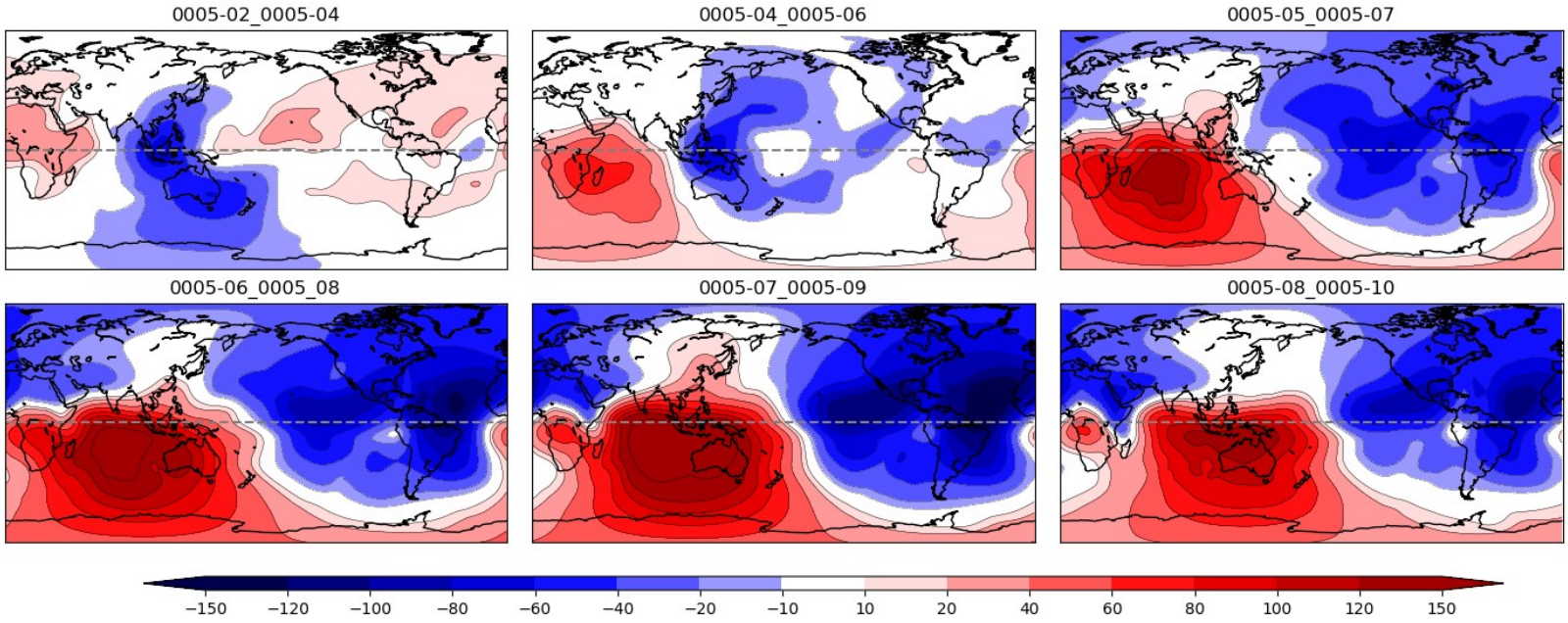

Figure 2. Velocity Potential anomalies at 200 hPa (10^ 6 m2 s-1) averaged over the periods (a) 0005-02 to 0005-04 (b) 0005-04 to0005-06 (c) 0005-05to 0005-07 (d) 0005-06 to 0005-08 (e) 0005-07 to 0005-09 (f) 0005-08 to 0005-10.

Once this wave of positive VP200 reaches the Western Pacific, it forms a standing wave pattern. Figure 3 shows the annually averaged VP200 anomalies starting with the year after the injection and ending 8 years following the injection, when the El Niño-like conditions begin to fade. A clear, persistent pattern of upper level convergence over the Western Pacific is present in the 150 Tg simulations for more than 7 years. This indicates that the Nuclear Niño is having impacts throughout the entire atmosphere. All surface based and upper level ENSO indices indicate a very strong El Niño is forced by nuclear conflict.

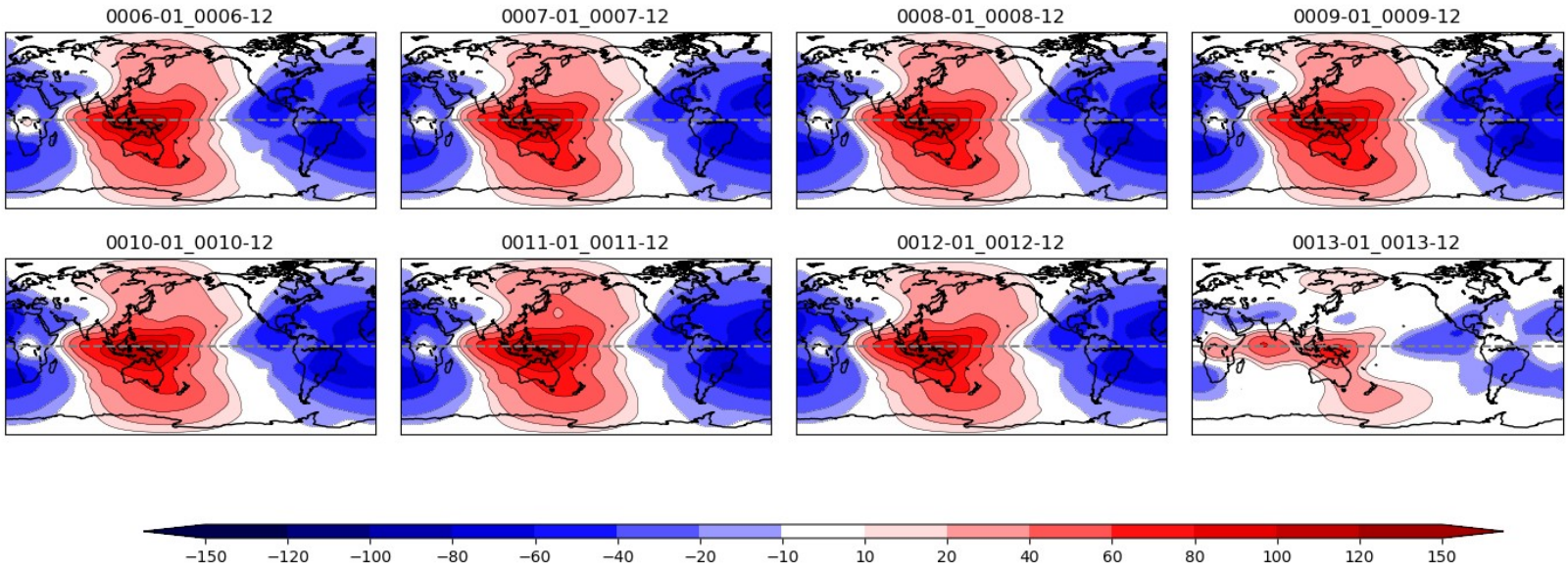

Figure 3. Velocity Potential anomalies at 200 hPa annually averaged over the periods (a) 0006-01 to 0006-12 (b) 0007-01 to 0007-12 (c) 0008-01 to 0008-12 (d) 0009-01 to 0009-12 (e) 0010-01 to 0010-12 (f) 0011-01 to 0011-12 (g) 0012-01 to 0012-12 (h) 0013-01 to 0013-12.

To be clear, Figure 4 shows VP200 anomalies which would be expected during a typical El Niño event (all months). The pattern simulated in the nuclear conflict runs are clearly representative of the upper level divergence pattern observed in a typical El Niño, and is in fact, much stronger. This pattern remains for years in the 150 Tg case, indicative of a strong impact of El Niño on the upper level (200 hPa) divergence pattern.

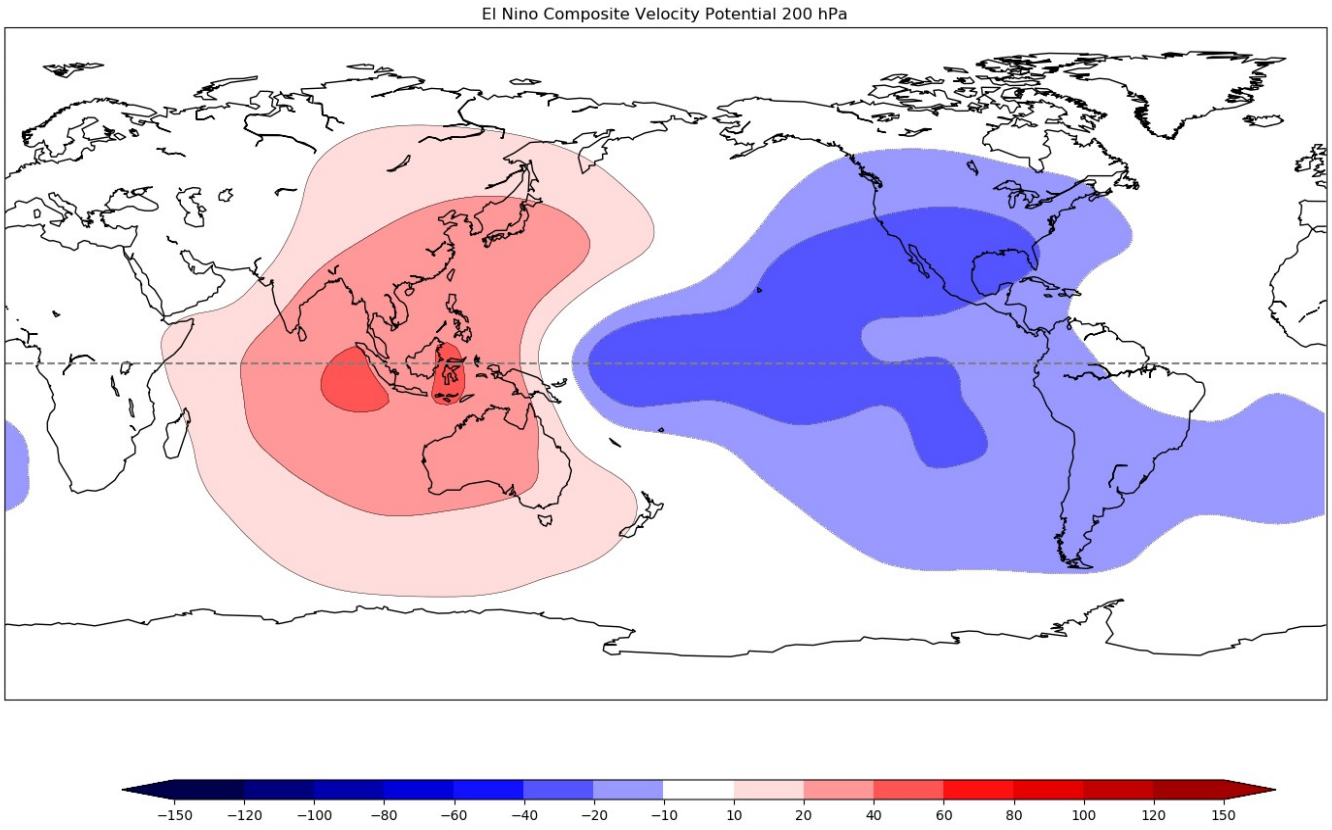

Figure 4. VP200 anomalies averaged over all El Niño months in the CESM1(WACCM4) control run.

References

Gill, E. C., B. Rajagopalan, and P. Molnar (2015), Subseasonal variations in spatial signatures of ENSO on the Indian summer monsoon from 1901 to 2009, J. Geophys. Res. Atmos., 120, 8165–8185, doi:10.1002/2015JD023184.